ORGANOMETALLICS

Article

pubs.acs.org/Organometallics

Rhodium-Catalyzed Selective Partial Hydrogenation of Alkynes

Jingwei Luo,[†] Robin Theron,[†] Laura J. Sewell,[‡] Thomas N. Hooper,[‡] Andrew S. Weller,[‡] Allen G. Oliver,[§] and J. Scott McIndoe*,[†]

[†]Department of Chemistry, University of Victoria, P.O. Box 3065, Victoria, BC V8W3 V6, Canada

[‡]Department of Chemistry, University of Oxford, Mansfield Road, Oxford, OX1 3TA, U.K.

[§]Molecular Structure Facility, Department of Chemistry and Biochemistry, University of Notre Dame, Notre Dame, Indiana 46556, United States

Supporting Information

ABSTRACT: The cationic rhodium complex $[Rh(P^cPr_3)_2(\eta^6\text{-PhF})]^+[B\{3,5\text{-}(CF_3)_2C_6H_3\}_4]^-$ (P^cPr_3 = triscyclopropylphosphine, PhF = fluorobenzene) was used as a catalyst for the hydrogenation of the charge-tagged alkyne $[Ph_3P(CH_2)_4C_2H]^+[PF_6]^-$. Pressurized sample infusion electrospray ionization mass spectrometry (PSI-ESI-MS) was used to monitor reaction progress. Experiments revealed that the reaction is first order in catalyst and first order in hydrogen, so under conditions of excess hydrogen the reaction is pseudo-zero order. Alkyne hydrogenation was 40 times faster than alkene hydrogenation. The turnover-limiting step is proposed to be oxidative addition of hydrogen to the alkyne (or alkene)-bound complex. Addition of triethylamine caused a dramatic reduction in rate, suggesting a deprotonation pathway was not operative.

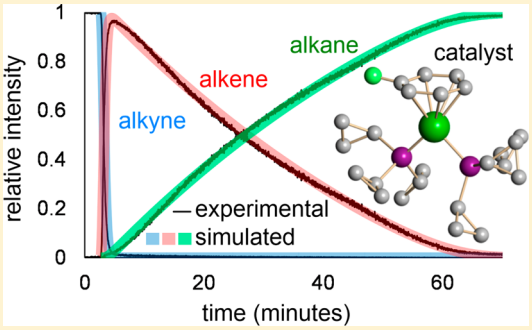

INTRODUCTION

Hydrogenation of alkynes and alkenes mediated by rhodium complexes is a classic catalytic organometallic reaction.[1] First introduced by Wilkinson,[2] the eponymous catalyst $Rh(PPh_3)_3Cl$ has been widely employed, thanks to the mild conditions it operates under and its selectivity for C−C multiple bonds over other unsaturated sites.[3] The mechanism of the reaction has been studied by a wide range of approaches.[4] It may well be *the* most well-studied organometallic catalytic reaction. It is relatively complicated, with off-cycle equilibria between catalyst monomer and dimer (and hydrogenated versions thereof) and between di- and triphosphine species. Cationic rhodium complexes are known for the hydrogenation of alkynes from Schrock and Osborn's work,[5] and since then, these types of complexes have served as precursors in various studies of homogeneous catalysis. Bis(ditertiaryphosphine) chelate complexes of rhodium(I) were studied as catalytic hydrogenators of methylenesuccinic acid, and cationic and hydrido versions of the complex were found to be more active than corresponding chloro versions, with activity increasing with increasing chain length of the diphosphine.[6a] Semihydrogenation of internal alkynes such as diphenylacetylene has also been developed with good selectivity with use of trinuclear cationic rhodium complexes.[6b] Innately linked to cationic rhodium hydrogenation is catalytic asymmetric synthesis to produce enantiomerically pure compounds due to the possibility of introducing a degree of chirality in the ligands on the metal center. Extensive work has been done in this area with rhodium and more recently with iridium and ruthenium complexes.[7] The scope of $[Rh(diene)(PR_3)_2]^+$ precursors[8] was further increased to the hydrogenation of imines,[9] and since then, the hydrogenations of prochiral imines for the production of a chiral amines has become a promising route for synthesis of chiral nitrogen-containing compounds.[10] DFT studies have become increasingly popular for the unravelling of mechanistic details of these systems.[11]

We have examined rhodium-catalyzed hydrogenation previously using electrospray ionization mass spectrometry (ESI-MS), wherein we doped in substoichiometric quantities of a charged phosphine ligand,[12] $[Ph_2P(CH_2)_4PPh_2Bn]^+[PF_6]^-$ (Bn = benzyl), into a reaction mixture consisting of an alkene, hydrogen, and Wilkinson's catalyst, using chlorobenzene as a solvent.[13] We observed a large variety of rhodium complexes consistent with the known speciation of this reaction mixture. However, because ESI-MS operates only on ions, the overall progress of the reaction was not tracked, and therefore the concentration of metal−ligand intermediates cannot be matched to activity. As such, establishing whether or not an observed species is an intermediate, a resting state, or a decomposition product is not easy. We later reexamined the reaction, where we added a charged tag to the substrate (in this case an alkyne) rather than the catalyst.[14] This paper confirmed that the turnover-limiting step was ligand dissociation from the precatalyst to generate the unsaturated, 14-electron species $Rh(PPh_3)_2Cl$. However, since all steps involving the alkyne on

Received: April 16, 2015
Published: June 9, 2015

DOI: 10.1021/acs.organomet.5b00322
Organometallics 2015, 34, 3021−3028

the metal were relatively fast, we saw no metal-containing intermediates during the reaction.

ESI-MS is increasingly popular as a method of establishing solution speciation in organometallic reactions.[15] It has been used on systems with inherently charged catalysts,[16] with neutral catalysts that become charged via oxidation[17] or protonation,[18] and with catalysts with deliberately charged ligands.[19] Use of charged substrates is somewhat rarer, as is continuous monitoring of reaction solutions, but we favor this approach thanks to the complete picture of speciation it provides.[20] Here, for the first time, we combine a charged substrate with a charged catalyst to allow simultaneous examination of the abundance and identity of all charged species in solution. Real-time monitoring of the charged species in solution was achieved using pressurized sample infusion ESI-MS (Figure 1).[21]

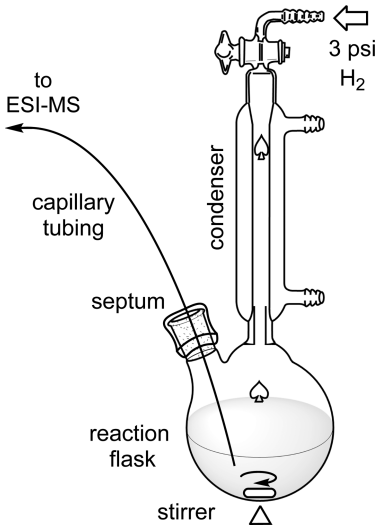

Figure 1. Pressurized sample infusion ESI-MS. The glassware used consisted of a Schlenk flask modified to incorporate a reflux condenser.

The cationic catalyst $[Rh(P^cPr_3)_2(\eta^6\text{-PhF})]^+[B\{3,5\text{-}(CF_3)_2C_6H_3\}_4]^-$ (**1**[BAr^F_4]; P^cPr_3 = triscyclopropylphosphine, PhF = fluorobenzene) was used, for which similar systems have been shown to be effective for both amine−borane dehydrocoupling reactions[22,23] and alkene hydroboration.[24] Cationic rhodium complexes are well known to be excellent selective hydrogenators of alkynes, from the classic work of Schrock and Osborn from the 1970s.[5] The charged alkyne substrate was $[Ph_3P(CH_2)_4C_2H]^+[PF_6]^-$ (**2**[PF_6]), which was hydrogenated over the course of the reaction to the alkene $[Ph_3P(CH_2)_4C(H){=}CH_2]^+[PF_6]^-$ (**3**[PF_6]) and eventually the alkane $[Ph_3P(CH_2)_5CH_3]^+[PF_6]^-$ (**4**[PF_6]). A slightly different alkene, $[Ph_3P(CH_2)_3C(H){=}CH_2]^+[PF_6]^-$ (**5**[PF_6]), was also prepared for a competition study.

EXPERIMENTAL SECTION

Fluorobenzene was freshly distilled from P_2O_5 before use. All other solvents were dispensed from an MBraun solvent purification system immediately before use. All reactions were under a nitrogen or argon atmosphere. Chemicals and solvents were purchased from Aldrich and used without subsequent purification. The charged alkyne was prepared by a previously published method.[1] All mass spectra were collected by using a Micromass Q-Tof Micro mass spectrometer in positive ion mode using pneumatically assisted electrospray ionization: capillary voltage, 3000 V; extraction voltage, 0.5 V; source temperature, 90 °C; desolvation temperature, 180 °C; cone gas flow, 100 L/h; desolvation gas flow, 100 L/h; collision voltage, 2 V (for MS experiments); collision voltage, 2−80 V (for MS/MS experiments); MCP voltage, 2700 V. Mass spectrometric interpretation was aided by ChemCalc.[25]

ESI-MS Reaction Monitoring Using Pressurized Sample Infusion. A Schlenk flask was used for these experiments, as shown in Figure 1. A 10 mL fluorobenzene solution of **2**[PF_6] (10−20 mg, 2.1−4.2 mM) was monitored using the pressurized sample infusion electrospray ionization mass spectrometry (PSI-ESI-MS) setup. The Schlenk flask was pressurized to 3 psi using 99.999% purity hydrogen gas. $[Rh(P^cPr_3)_2(\eta^6\text{-FPh})]^+[BAr^F_4]^-$ (1.0−6.0 mg, 0.75−4.5 μmol, 1−20% catalyst loading) was dissolved in 1 mL of fluorobenzene and injected into the well-stirred Schlenk flask via a septum. The solution end of the PEEK tubing was protected with a standard cannula filter system to avoid the tube being blocked by any insoluble byproducts. Data were processed by normalizing the abundance of each species to the total ion count of all species identified as containing the tag. No smoothing of the data was performed. The triethylamine reaction was conducted using 2.2 mM of the charged alkyne, 0.22 mM of the catalyst, and 1.12 mM of NEt_3. The reaction with D_2 used the same overpressure as for H_2.

1[BAr^F_4]: [$Rh(P^cPr_3)_2(\eta^6\text{-}C_6H_5F)]^+[BAr^F_4]^-$. $[RhCl(P^cPr_3)_2]_2$ was prepared by the procedure described by Goldman et al.[26] $[RhCl(P^cPr_3)_2]_2$ (0.100 g, 0.112 mmol) and $Na[BAr^F_4]$ (0.203 g, 0.229 mmol) were added to a Schlenk flask, and fluorobenzene (5 cm^3) was added. After stirring for 1 h the solution was filtered, and the volume was reduced *in vacuo* to approximately 2 cm^3. This solution was layered with *n*-pentane (20 cm^3), and storage at room temperature gave $[Rh(P^cPr_3)_2(\eta^6\text{-}C_6H_5F)][BAr^F_4]$ as brown crystals (0.200 g, 65%) after 48 h. ^{1}H NMR (C_6H_5F, 500 MHz): 8.38 (s, 8H, BAr^F_4), 7.69 (s, 4H, BAr^F_4), 6.20 (m, 2H, C_6H_5F), 6.12 (m, 2H, C_6H_5F), 5.68 (m, 1H, C_6H_5F), 0.60 (br m, 24H, ^{c}Pr CH_2), 0.36 (br m, 6H, ^{c}Pr CH) ppm. $^{31}P\{^1H\}$ NMR (C_6H_5F, 202 MHz): 41.4 (d, $^1J_{PRh}$ = 206 Hz) ppm. Anal. Calcd for $C_{56}H_{47}BF_{25}P_2Rh$ (1370.60 g mol^{-1}): C, 49.07; H, 3.46. Found: C, 48.84; H, 3.39. ESI-MS(+) (C_6H_5F, 60 °C): *m*/*z* 507.12.

2[I]: [$Ph_3P(CH_2)_4C_2H]^+[I]^-$, Hex-5-yn-1-yltriphenylphosphonium Iodide. Triphenylphosphine (5.00 g, 19.0 mmol) was dissolved into 10 mL of toluene in a Schlenk flask at 75 °C, and 6-iodo-1-hexyne (1.00 g, 4.81 mmol) added dropwise over 10 min. The mixture was stirred for 72 h, before the product was filtered off, washed with toluene, and dried under high vacuum. Final product was a white powder (2.22 g, 4.72 mmol, 98%). Crystals for X-ray crystallographic analysis were grown by vapor diffusion of hexane into a chloroform solution. ESI-MS(+): *m*/*z* 343.1. ESI-MS(−): *m*/*z* 126.9.

2[PF_6]: [$Ph_3P(CH_2)_4C_2H]^+[PF_6]^-$, Hex-5-yn-1-yltriphenylphosphonium Hexafluorophosphate(V). Sodium hexafluorophosphate (0.56 g, 2.12 mmol) was dissolved in 5 mL of water, and 5 mL of a methanol/water mixed solution of $[Ph_3P(CH_2)_4C_2H]^+[I]^-$ (0.5 g 1.06 mmol) was added dropwise with stirring. The product was filtered and washed with water and dried under high vacuum for a week. Final product was a white powder (0.55 g, 1.12 mmol, 53%). ^{1}H NMR ($CDCl_3$ 300 MHz): δ (ppm) 7.81 (m, 3H, PPh_3); 7.70 (m, 12H, PPh_3); 3.22 (m, 2H, PPh_3CH_2); 2.29 (m, 2H, CH_2C_2H); 1.86, (t, 1H, $CH_2CH_2CH_2C_2H$); 1.81 (m, 3H, $CH_2CH_2CH_2C_2H$); 1.26 (s, 1H, C_2H). ESI-MS(+): *m*/*z* 343.1. ESI-MS(−): *m*/*z* 145.0.

5[I]: [$Ph_3P(CH_2)_3C(H){=}CH_2]^+[PF_6]^-$, Pent-4-en-1-yltriphenylphosphonium Bromide. Triphenylphosphine (5.5 g, 20.1 mmol) was dissolved into 10 mL of toluene in a Schlenk flask at 75 °C, and 5-bromo-1-pentene (2.1 g, 13.4 mmol) added dropwise over 10 min. The mixture was stirred for 72 h, before the product was filtered off, washed with toluene, and dried under high vacuum. Final product was a white powder (0.50 g, 1.2 mmol, 9%). ESI-MS(+): *m*/*z* 331.1. ESI-MS(−): *m*/*z* 78.9.

5[PF_6]: [$Ph_3P(CH_2)_3C(H){=}CH_2]^+[PF_6]^-$, Pent-4-en-1-yltriphenylphosphonium Hexafluorophosphate(V). Sodium hexafluorophosphate (0.50 g, 3.0 mmol) was dissolved in 5 mL of water, and 5 mL of a water solution of $[Ph_3P(CH_2)_3C_2H_3]^+[I]^-$ (0.50 g, 1.2 mmol) was added dropwise with stirring. The product was filtered and washed with water and dried under high vacuum for a week. Final product was

DOI: 10.1021/acs.organomet.5b00322
Organometallics 2015, 34, 3021−3028

a white powder (0.52 g, 1.1 mmol, 91%). ^{1}H NMR ($CDCl_3$ 300 MHz): δ (ppm) 7.80 (m, 3H, PPh_3); 7.68 (m, 12H, PPh_3); 5.68 (m, 1H, $-CH_2CH_2$); 5.05 (m, 2H, $-CH_2CH_2$); 3.13 (m, 2H, PPh_3CH_2); 2.30 (m, 2H, $-CH_2CH_2CH_2$); 1.71 (m, 2H, $PPh_3CH_2CH_2$). ESI-MS(+): m/z 331.1. ESI-MS(−): m/z 145.0.

RESULTS AND DISCUSSION

Cationic rhodium(I) complexes are, as already mentioned, known to be active hydrogenation catalysts[27] and are readily detected by ESI-MS. Used here was $[Rh(P^cPr_3)_2(\eta^6\text{-FPh})]^+[BAr^F{}_4]^-$ (Ar^F = 3,5-bis(trifluoromethyl)phenyl) (**1**[$BAr^F{}_4$]),[15] as the phosphine is small, tied-back, and unlikely to partake in C−H activation or intramolecular dehydrogenation reactions that would complicate the mass spectral analysis. The charged substrate used was $[Ph_3P(CH_2)_4C_2H]^+[PF_6]^-$ (**2**[PF_6]), which proved to have the right combination of solubility, high ESI-MS response factor, and lack of reactivity of the tag for the purposes of reaction analysis.[14] The product alkane, $[Ph_3P(CH_2)_5CH_3][PF_6]$ (**4**[PF_6]), was isolated and crystallized to establish that the reactivity of the charge-tagged alkyne duplicates that of a regular terminal alkyne; the resulting structure of the triphenylhexylphosphonium salt was entirely unremarkable (Figure 2).

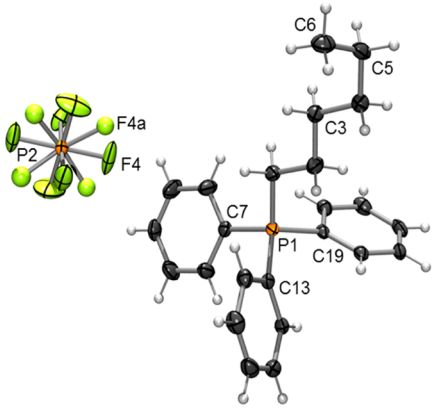

Figure 2. Alkane hydrogenation product **4**[PF_6]. Key bond lengths and angles: C5−C6 1.499(3) Å; C4−C5−C6 113.86(19)°.

The kinetic profile of the alkyne hydrogenation reaction proved to be very different from that catalyzed by Wilkinson's catalyst, $Rh(PPh_3)_3Cl$.[1] For Wilkinson's catalyst, the rate of alkyne hydrogenation was only 3 times faster than the rate of alkene hydrogenation, and the turnover-limiting step was phosphine dissociation from the $Rh(PPh_3)_3Cl$ precatalyst to generate the reactive 14-electron species $Rh(PPh_3)_2Cl$. However, for the cationic rhodium catalyst studied here, hydrogenation of the alkyne $\mathbf{2}^+$ was 40× faster than hydrogenation of the corresponding alkene, $[Ph_3P(CH_2)_4CH{=}CH_2]^+$ ($\mathbf{3}^+$), and production of both appeared to be essentially zero order in alkyne (alkene). No intermediates were observed that included both rhodium complex and the charged tag, and the only observed rhodium-containing species were $[Rh(P^cPr_3)_2(\eta^6\text{-FPh})]^+$ ($\mathbf{1}^+$) and $[Rh(P^cPr_3)_2]^+$ ($\mathbf{1a}^+$). These features are summarized in Figure 3.

The selectivity for alkyne over alkene is striking at the early stages of reaction (at least 40:1), but because the reaction is (close to) zero order in alkynes (alkene), we suspect that this

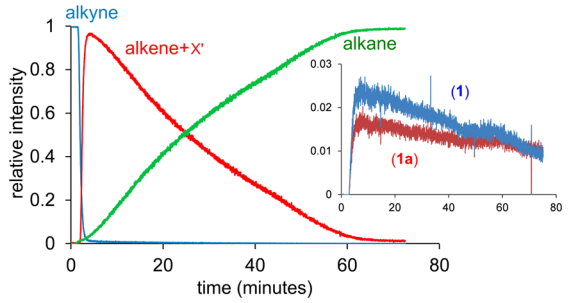

Figure 3. PSI-ESI-MS trace for hydrogenation of the alkyne **2**[PF_6] under 3 psi of H_2, with 13.3% of **1**[$BAr^F{}_4$] as catalyst at room temperature with FPh as solvent. Inset: Relative intensity vs time plot exhibiting behavior of $[Rh(P^cPr_3)_2(\eta^6\text{-FPh})]^+$ ($\mathbf{1}^+$) and $[Rh(P^cPr_3)_2]^+$ ($\mathbf{1a}^+$).

substrate is not involved in the turnover-limiting step (*vide infra*). This suggests that the alkyne (alkene) coordination to the Rh complex is fast and lies a long way toward the alkyne (or alkene) complex, but that the alkyne still substantially outcompetes the alkene. The reaction is sensitive to the temperature it is run at (Figure 4), confirming that the reaction is taking place in solution rather than being some sort of artifact of the ESI-MS ionization process.[28]

The reaction is first order in catalyst concentration (see Supporting Information), there is no induction period, and no

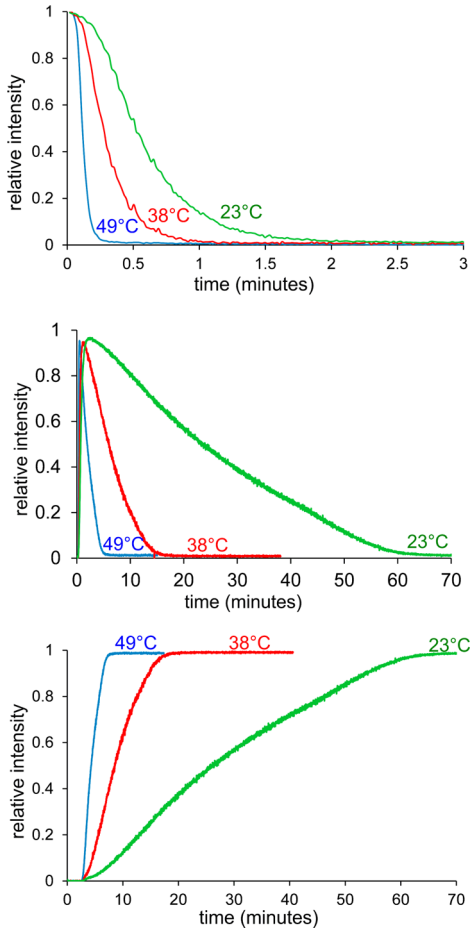

Figure 4. PSI-ESI-MS traces for (top) the disappearance of alkyne $\mathbf{2}^+$ at 23, 38, and 49 °C (fast at all temperatures); (middle) appearance and consumption of alkene $\mathbf{3}^+$; (bottom) appearance of alkane $\mathbf{4}^+$.

DOI: 10.1021/acs.organomet.5b00322
Organometallics 2015, 34, 3021−3028

di- or polynuclear rhodium species are observed, suggesting that the reaction involves a mononuclear rhodium species as catalyst. Hydrogen was present in large excess during the preliminary catalytic runs, so another experiment was carried out to establish whether the reaction profile changed under stoichiometric conditions. The experiment was reexamined using a single equivalent of H_2 (170 μL); the (well-stirred, to avoid diffusion effects) reaction was much slower, and the overall reaction displayed first-order characteristics (Figure 5).

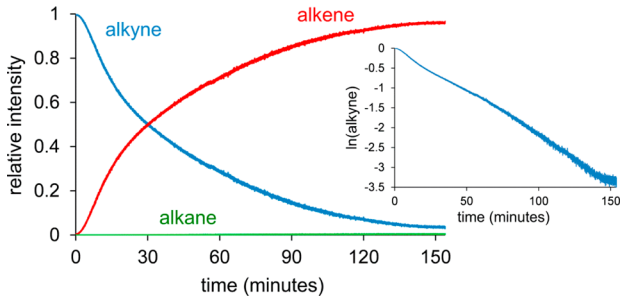

Figure 5. PSI-ESI-MS traces for the selective hydrogenation of the charge-tagged alkyne $\mathbf{2}^+$ in the presence of 1.1 equiv of H_2. Inset: ln[x] vs time plot exhibiting first-order behavior.

The reaction rate doubled if two equivalents of H_2 were used instead of one (see the Supporting Information), suggesting the reaction is not limited by mass transport under these experimental conditions.

Given that the turnover-limiting step seemed to involve hydrogen, it was reasonable to assume that a primary kinetic isotope effect (KIE)[29] may be detectable in the reaction. As such, the reaction was examined using D_2 instead of H_2, and we found the alkene → alkane reduction to be appreciably faster for H_2, by a factor of $k_H/k_D = 2.1 \pm 0.2$ (Figure 6). This value is

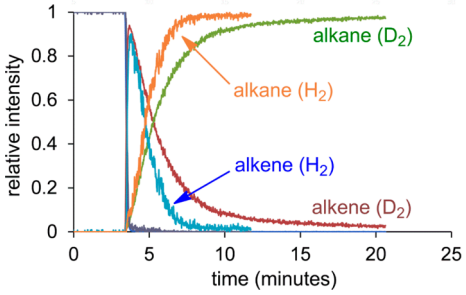

Figure 6. PSI-ESI-MS traces for the reduction of alkyne $\mathbf{2}^+$ to alkane $\mathbf{4}^+$ using H_2 (blue/yellow) vs D_2 (green/red).

consistent with oxidative addition (OA) being the slow step, since concerted OA requires the breaking of a H−H (D−D) bond. This KIE is larger than expected if hydride insertion or reductive elimination was rate-determining.[30] We cannot discount that equilibrium isotope effects are operating prior to such a step, and reactions involving small molecules such as H_2 can generate isotope effects that are highly dependent on system and temperature.[31] However, other evidence points to H_2 addition after alkyne (or alkene) binding being turnover-limiting (*vide infra*).

So while the kinetics point to the oxidative addition of H_2 being turnover-limiting, the fact we are unable to identify intermediates by ESI-MS containing the charge-tagged alkyne or the alkene needs justifying. We can do so on several grounds:

(a) Monodentate alky(e)nes are difficult to characterize by ESI-MS at the best of times because they are generally weakly bound and easily lost during the desolvation process.[13] This is exacerbated for a cationic metal complex binding a cationic alky(e)ne, as the charges repel each other.

(b) Addition of octyne to $\mathbf{1}[BAr^F{}_4]$ displaces the fluorobenzene and produces the ions $[Rh(P^cPr_3)_2(octyne)_n]^+$ (n = 1 or 2; see Supporting Information). This observation suggests that fluorobenzene is a relatively weakly bound ligand[32] and is easily displaced by alkynes. Interestingly, with different, chelating, ligands and CH_2Cl_2 solvent PhF dissociation is slow.[33]

(c) We never observe ions of the form $[Rh(P^cPr_3)(H)_2]^+$ in the mass spectrometer in the presence of H_2, suggesting that addition of H_2 to the catalyst is either slow or lies a long way in the wrong direction (hydrides are readily observed by ESI-MS).[34] We examined complex $\mathbf{1}[BAr^F{}_4]$ with ^1H and $^{31}P\{^1H\}$ NMR spectroscopy under a pressure of ∼4 atm of H_2 in PhF solvent, and there were no observable changes at room temperature (storage of this solution under H_2 overnight led to the appearance of a doublet of multiplets at δ 4.33 ppm ($^2J_{HF}$ = 48.8 Hz) and several multiplets from δ 1.68 to 0.73 ppm characteristic of fluorocyclohexane[35] from the hydrogenation of fluorobenzene, a process that has been shown previously to proceed via a colloidal Rh catalytic route[36]). By contrast, addition of alkyne (1-octyne) to a PhF solution of $\mathbf{1}[BAr^F{}_4]$ at 5 mol % loadings resulted in complex $^{31}P\{^1H\}$ and ^1H NMR spectra that showed many species to be present. No distinctive signals at high field in the ^1H NMR spectrum that would indicate Rh−H species were observed. Addition of 1-octyne to a sample of $\mathbf{1}[BAr^F{}_4]$ under 4 atm of H_2 led to very similar $^{31}P\{^1H\}$ and ^1H NMR spectra, suggesting similar speciation under H_2. 1-Octene was also observed, consistent with catalytic turnover. These NMR data suggest that H_2 addition is the limiting rate, and thus the complex speciation observed by solution NMR spectroscopy represents the resting state of the system.

Osborn and Schrock outlined three possible mechanisms for the hydrogenation of alkenes by cationic rhodium complexes (Scheme 1).[5]

Path A involved addition of H_2 to $[RhL_n]^+$, then deprotonation to form an active neutral catalyst of the form $HRhL_n$. Alkene coordination, migration, H_2 addition, and reductive elimination of alkane followed. Path B involved addition of H_2, then coordination of alkene to $[RhL_n]^+$, followed by migration and reductive elimination of the product alkane. Path C is the same as path B, except the order of H_2 and alkene addition is reversed. Osborn and Schrock considered path A to predominate in the polar solvents acetone, 2-methoxyethanol, and tetrahydrofuran, except where binding of the alkene was particularly strong, such as in the selective hydrogenation of dienes.[5] THF is capable of deprotonating metal hydrides.[37]

Halpern and co-workers studied hydrogenation of 1-hexene and other substrates using a variety of $[Rh(PP)]^+$ (PP = chelating bisphosphine) complexes as catalysts under mild conditions in methanol (ambient temperature and 1 atm of H_2).[38] They found that oxidative addition of H_2 to $[Rh(PP)(alkene)]^+$ was rate-determining, consistent with pathway C being operative. They found that the bis(triphenylphosphine) complex seemed to proceed via pathway B, with the slow steps

DOI: 10.1021/acs.organomet.5b00322
Organometallics 2015, 34, 3021−3028

Scheme 1. Pathways for Alkene Hydrogenation, after Schrock and Osborn[5]

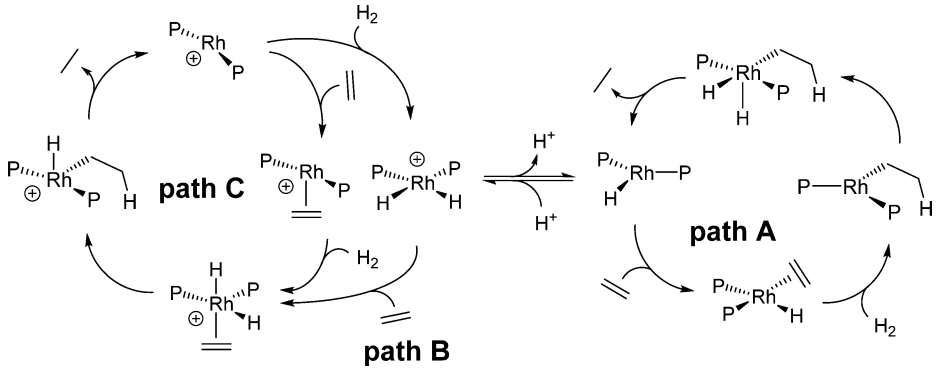

being addition of the alkene to $[H_2Rh(PPh_3)_2]^+$ and elimination of the alkane, but that the observed kinetics were also consistent with pathway C if oxidative addition of H_2 was fast and the equilibrium lay a long way to the product.[39]

We considered all three mechanisms as possible candidates to explain our observations, but ultimately settled on path C, for the following reasons:

(a) Neither $HRhL_n$ (path A) nor $[H_2RhL_n]^+$ (path B) could be detected by ^1H NMR spectroscopy when examining $[RhP_2(\eta^6\text{-FPh})]^+$ in the presence of H_2, nor could $[H_2RhL_n]^+$ (path B) be observed by ESI-MS. If path B is operative, the equilibrium must lie a long way toward the left.

(b) If path A was operative, any of the intermediates $HRhP_2$(alkene), $RhRP_2$, and RhH_2RP_2 would be expected to be observable as monocations using ESI-MS, due to the charged tag. None of these species were in fact observed. If this path was operative, at least one (the resting state) should be seen.

(c) Addition of bases such as NEt_3 ought to accelerate reactions proceeding through a fast path A, due to the deprotonation equilibrium being perturbed in the direction of $RhHP_2$. However, no such acceleration was observed. Indeed, the reaction was *slowed* in the presence of NEt_3 (Figure 7), and the reaction became much less selective for the alkyne.

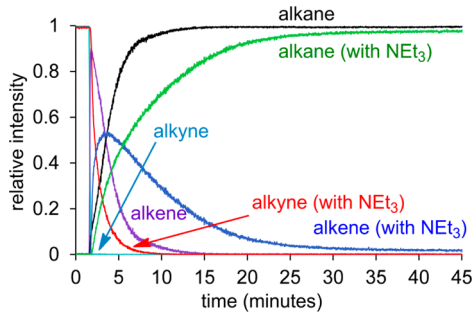

Figure 7. PSI-ESI-MS traces showing the effect of NEt_3 on the rate and selectivity of hydrogenation.

The reaction reached a maximum of 50% in alkene only, very similar to the degree of selectivity exhibited by Wilkinson's catalyst.[1] Addition of NEt_3 to $[RhP_2]^+$ in the presence of H_2 resulted in disappearance of $[RhP_2]^+$ and the appearance of $[HNEt_3]^+$ (see the Supporting Information), suggesting the formation of neutral $RhHP_2$ and the operation of the slower and less alkyne-selective path A.

(d) The solvent used, fluorobenzene, is inimical to deprotonation compared to the polar solvents used by Schrock and Osborn (tetrahydrofuran, acetone, 2-methoxyethanol).

(e) The numerical modeling (*vide infra*) proved most tractable for path C, providing excellent correlation with experimental data. Neither path A nor path B provided sensible solutions. This evidence is circumstantial given that the fit of eight rate constants is underdetermined, but nonetheless it confirms that there exist plausible sets of rate constants for path C that fit nicely to the experimental data. Path C has been redrawn in Scheme 2 and elaborated to include the alkyne and the alkene on the same plot.

Scheme 2. Mechanism of Alkyne/Alkene Hydrogenation[a]

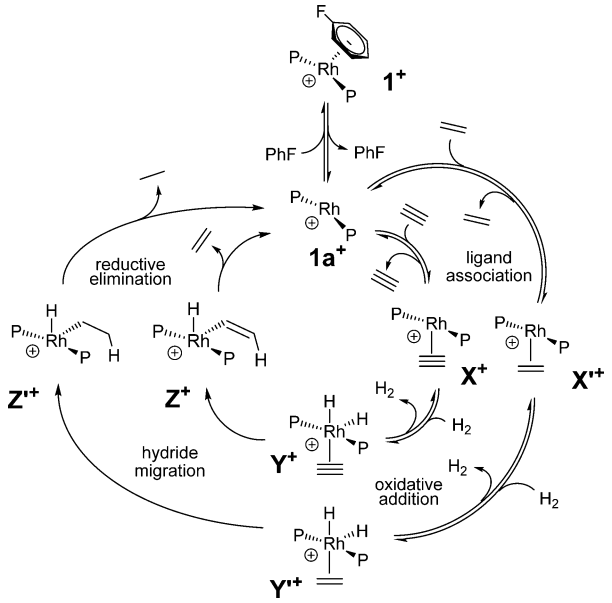

[a]P = P(cyclopropyl)$_3$.

Using the cycle in Scheme 2, we constructed a numerical model and used the program COPASI[40] to generate a set of rate constants compatible with the results that we observe. We then tested a variety of optimization methods and starting points. Given the number of independent parameters (if all steps in the cycle were reversible, there are 18 rate constants to consider), we simplified the picture by assuming hydride migration and reductive elimination steps were fast and (quasi) irreversible, leaving a more tractable 10 rate constants to optimize. Two out of these 10 rate constants, $\mathbf{1}^+ \rightarrow \mathbf{1a}^+$ and $\mathbf{1a}^+$

DOI: 10.1021/acs.organomet.5b00322
Organometallics 2015, 34, 3021−3028

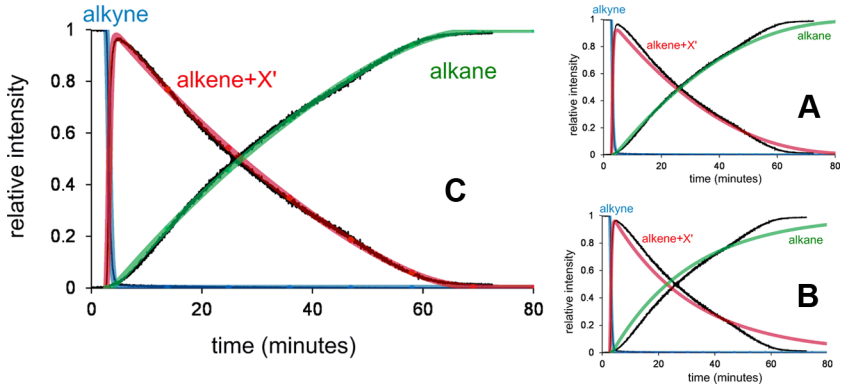

Figure 8. Direct comparison between simulated (colored lines) and experimental results (black, from PSI-ESI-MS) for path C and, in the inset, paths A and B.

→ $\mathbf{1}^+$, can be approximated based on the experimental measurements. These showed that a stable amount of $\mathbf{1a}^+$ exists in the reacting solution. After we fix these values to produce the roughly equivalent amounts of $\mathbf{1}^+$ and $\mathbf{1a}^+$ as seen in the ESI-MS traces, the remaining eight rate constants can be optimized by COPASI by using a variety of mathematical methods (see the Supporting Information). All these methods generated similar rate constants and high-quality matches for the experimental data for path C. Similar procedures carried out with paths A and B produce significantly worse matches, being unable to replicate the close to zero-order behavior or the significant quantities of $\mathbf{1}^+$ and $\mathbf{1a}^+$ present throughout the reaction (Figure 8).

The lack of any initiation time suggested that fluorobenzene dissociation ($\mathbf{1}^+ \rightarrow \mathbf{1a}^+$) was fast. As such, trying to model this dissociation step added complexity to the model without adding anything to our understanding of the productive part of the cycle. Accordingly, we inspected the catalyst behavior over the course of the reaction and selected rate constants that reflected the relative abundances of $\mathbf{1}^+$ and $\mathbf{1a}^+$. These values were approximated to 10 min^{-1} and 0.1 min^{-1} $mmol^{-1}$ L, respectively. All models predicted that binding of the alkene to $\mathbf{1a}^+$ was slower than the binding of the alkyne to $\mathbf{1a}^+$ ($\mathbf{1a}^+ \rightarrow \mathbf{X}^+$) by a factor of at about 40, but that both were relatively fast. However, this factor appeared to be just part of the reason for the selectivity for alkyne over alkene. Oxidative addition of hydrogen ($\mathbf{X}^+ \rightarrow \mathbf{Y}^+$) seems to be turnover-limiting, as predicted by the stoichiometric H_2 addition, the overall zero-order kinetics, and the primary KIE established from the D_2 experiment. As expected, the numerical modeling is in agreement: this step is slow and, especially so for the alkene, by a factor of about 40 compared to the alkyne. No attempt was made to model the migration and reductive elimination ($\mathbf{Y}^+ \rightarrow \mathbf{Z}^+$ and $\mathbf{Z}^+ \rightarrow \mathbf{1a}^+$) steps. $\mathbf{Y}^+$ and $\mathbf{Z}^+$ are indistinguishable by MS because they are isomers, and the fact that neither could be observed makes it unlikely that they are resting states.

Further confirmation of the mechanism came through competition experiments. We took the charge-tagged alkyne $\mathbf{2}[PF_6]$ and a similar charge-tagged alkene, $\mathbf{5}[PF_6]$, and conducted an excess H_2 reduction competitively. Neither alkene ($\mathbf{3}[PF_6]$ as derived from $\mathbf{2}[PF_6]$ or $\mathbf{5}[PF_6]$) reacted until practically all of the alkyne $\mathbf{2}[PF_6]$ was consumed, at which point the observed rates of alkene consumption were fairly similar to each other (Supporting Information): 3.2×10^{-4} mol L^{-1} min^{-1} for $\mathbf{5}[PF_6]$ + H_2 and 2.5×10^{-4} mol L^{-1} min^{-1} for $\mathbf{3}[PF_6]$ + H_2. The fractionally faster rate for $[Ph_3P(CH_2)_3CH{=}CH_2]^+$ was perhaps due to a small electronic effect due to the greater proximity of the charged tag.

Examination of catalyst behavior showed that the ratio of $\mathbf{1}^+$ to $\mathbf{1a}^+$ stayed fairly constant and fairly similar in intensity throughout the reaction (see the Supporting Information). The absolute intensity reached a maximum soon after catalyst addition, and the intensity drops as the reaction proceeds, stabilizing at the completion of the reaction. We attribute this behavior to a competitive catalyst decomposition pathway stemming from a reaction intermediate (if the decomposition was from a catalyst precursor, the decomposition ought to continue after the cessation of the reaction). We could not identify any charged rhodium-containing species that could account for the disappearance of signal, suggesting that the decomposition product is neutral. RhP_2H is one such possibility; there was no color change that might indicate the formation of metallic rhodium.

CONCLUSIONS

Analysis of alkyne hydrogenation using a charge-tagged alkyne and a cationic rhodium catalyst revealed the catalyst to be a highly efficient partial hydrogenator, with a rate of alkyne hydrogenation in excess of 40 times faster than alkene hydrogenation. The mechanism was shown by a combination of ESI-MS, NMR, kinetic isotope effects, and numerical modeling methods to most likely have a turnover-limiting step of oxidative addition of hydrogen following alkyne/alkene binding. Using a stoichiometric amount of hydrogen was shown to be an effective means of enabling selective hydrogenation to the alkene.

ASSOCIATED CONTENT

Supporting Information

Numerical modeling, further kinetic data, mass spectra, X-ray crystal structure data for precatalyst $\mathbf{1}[BAr^F{}_4]$. The Supporting Information is available free of charge on the ACS Publications website at DOI: 10.1021/acs.organomet.5b00322.

AUTHOR INFORMATION

Corresponding Author

*Fax: +1 (250) 721-7147. Tel: +1 (250) 721-7181. E-mail: mcindoe@uvic.ca.

Notes

The authors declare no competing financial interest.

DOI: 10.1021/acs.organomet.5b00322
Organometallics 2015, 34, 3021−3028

■ ACKNOWLEDGMENTS

J.S.M. thanks the Natural Sciences and Engineering Research Council (NSERC) of Canada, the Canada Foundation for Innovation (CFI), the British Columbia Knowledge Development Fund (BCKDF), and the University of Victoria for instrumentation and operational funding. A.S.W. thanks the University of Oxford and the EPSRC (EP/J02127X/1).

■ REFERENCES

(1) (a) James, B. R. *Homogeneous Hydrogenation*; Wiley: New York, 1973. (b) Hartwig, J. F. *OrganoTransition Metal Chemistry*; University Science Books: Sausalito, CA, 2010.
(2) Young, J. F.; Osborn, J. A.; Jardine, F. H.; Wilkinson, G. *Chem. Commun.* **1965**, 131−132.
(3) Osborn, J. A.; Jardine, F. H.; Young, J. F.; Wilkinson, G. *J. Chem. Soc. A* **1966**, 1711−1732.
(4) (a) Halpern, J.; Okamoto, T.; Zakhariev, A. *J. Mol. Catal.* **1977**, *2*, 65−68. (b) Cabrera, M. I.; Zgolicz, P. D.; Grau, R. J. *Appl. Catal. A: Gen.* **2008**, *334*, 291−303. (c) Nelson, D. J.; Li, R.; Brammer, C. *J. Org. Chem.* **2004**, *70*, 761−767. (d) Bowker, M.; Gland, J.; Joyner, R.; Li, Y.; Slin'ko, M.; Whyman, R. *Catal. Lett.* **1994**, *25*, 293−308. (e) Koga, N.; Daniel, C.; Han, J.; Fu, X. Y.; Morokuma, K. *J. Am. Chem. Soc.* **1987**, *109*, 3455−3456. (f) Wink, D.; Ford, P. C. *J. Am. Chem. Soc.* **1985**, *107*, 1794−1796. (g) Wink, D. A.; Ford, P. C. *J. Am. Chem. Soc.* **1987**, *109*, 436−442. (h) Duckett, S. B.; Newell, C. L.; Eisenberg, R. *J. Am. Chem. Soc.* **1993**, *115*, 1156−1157. (i) Duckett, S. B.; Newell, C. L.; Eisenberg, R. *J. Am. Chem. Soc.* **1994**, *116*, 10548−10556.
(5) Schrock, R. R.; Osborn, J. A. *J. Am. Chem. Soc.* **1976**, *98*, 2143−2147.
(6) (a) James, B. R.; Mahajan, D. *Can. J. Chem.* **1979**, *57*, 180−187. (b) Kohrt, C.; Wienhöfer, G.; Pribbenow, C.; Beller, M.; Heller, D. *ChemCatChem* **2013**, *5*, 2818−2821.
(7) (a) James, B. R.; Wang, D. K. W. *Can. J. Chem.* **1980**, *58*, 245−250. (b) Knowles, W. S. *Adv. Synth. Catal.* **2003**, *345*, 3−13. (c) Cipot, J.; McDonald, R.; Ferguson, M. J.; Schatte, G.; Stradiotto, M. *Organometallics* **2007**, *26*, 594−608. (d) Bell, S.; Wüstenberg, B.; Kaiser, S.; Menges, F.; Netscher, T.; Pfaltz, A. *Science* **2006**, *311*, 642−644.
(8) Chan, A. S. C.; Pluth, J. J.; Halpern, J. *Inorg. Chim. Acta* **1979**, *37*, L477−L479.
(9) (a) James, B. R. *Catal. Today* **1997**, *37*, 209−221. (b) Kobayashi, S.; Ishitani, H. *Chem. Rev.* **1999**, *99*, 1069−1094.
(10) Longley, C. J.; Goodwin, T. J.; Wilkinson, G. *Polyhedron* **1986**, *5*, 1625−1628.
(11) (a) Landis, C. R.; Hilfenhaus, P.; Feldgus, S. *J. Am. Chem. Soc.* **1999**, *121*, 8741−8754. (b) Imamoto, T.; Tamura, K.; Zhang, Z.; Horiuchi, Y.; Sugiya, M.; Yoshida, K.; Yanagisawa, A.; Gridnev, I. D. *J. Am. Chem. Soc.* **2012**, *134*, 1754−1769. (c) Donald, S. M. A.; Vidal-Ferran, A.; Maseras, F. *Can. J. Chem.* **2009**, *87*, 1273−1279. (d) Reetz, M. T.; Meiswinkel, A.; Mehler, G.; Angermund, K.; Graf, M.; Thiel, W.; Mynott, R.; Blackmond, D. G. *J. Am. Chem. Soc.* **2005**, *127*, 10305−10313.
(12) Chisholm, D. M.; McIndoe, J. S. *Dalton Trans.* **2008**, 3933−3945.
(13) Chisholm, D. M.; Oliver, A. G.; McIndoe, J. S. *Dalton Trans.* **2010**, *39*, 364−373.
(14) Luo, J.; Oliver, A. G.; McIndoe, J. S. *Dalton Trans.* **2013**, *42*, 11312−11318.
(15) (a) Hývl, J.; Roithová, J. *Org. Lett.* **2013**, *16*, 200−203. (b) Chen, P. *Angew. Chem., Int. Ed.* **2003**, *42*, 2832−2847. (c) Torker, S.; Merki, D.; Chen, P. *J. Am. Chem. Soc.* **2008**, *130*, 4808−4814. (d) Santos, L. S. *Eur. J. Org. Chem.* **2008**, *2008*, 235−253. (e) Eberlin, M. *Eur. J. Mass Spectrom.* **2007**, *13*, 19−28. (f) Robinson, P. S. D.; Khairallah, G. N.; da Silva, G.; Lioe, H.; O'Hair, R. A. J. *Angew. Chem., Int. Ed.* **2012**, *51*, 3812−3817. (g) Ryzhov, V.; Lam, A. Y.; O'Hair, R. J. *J. Am. Soc. Mass Spectrom.* **2009**, *20*, 985−995. (h) Vikse, K. L.; Ahmadi, Z.; Manning, C. C.; Harrington, D. A.; McIndoe, J. S. *Angew. Chem., Int. Ed.* **2011**, *50*, 8304−8306. (i) Schade, M. A.; Fleckenstein, J. E.; Knochel, P.; Koszinowski, K. *J. Org. Chem.* **2010**, *75*, 6848−6857. (j) Jansen, H.; Samuels, M. C.; Couzijn, E. P. A.; Slootweg, J. C.; Ehlers, A. W.; Chen, P.; Lammertsma, K. *Chem.—Eur. J.* **2010**, *16*, 1454−1458. (k) dos Santos, M. R.; Coriolano, R.; Godoi, M. N.; Monteiro, A. L.; de Oliveira, H. C. B.; Eberlin, M. N.; Neto, B. A. D. *New J. Chem.* **2014**, *38*, 2958−2963. (l) Medeiros, G. A.; da Silva, W. A.; Bataglion, G. A.; Ferreira, D. A. C.; de Oliveira, H. C. B.; Eberlin, M. N.; Neto, B. A. D. *Chem. Commun.* **2014**, *50*, 338−340. (m) Oliveira, F. F. D.; dos Santos, M. R.; Lalli, P. M.; Schmidt, E. M.; Bakuzis, P.; Lapis, A. A. M.; Monteiro, A. L.; Eberlin, M. N.; Neto, B. A. D. *J. Org. Chem.* **2011**, *76*, 10140−10147.
(16) (a) Banu, L.; Blagojevic, V.; Bohme, D. K. *J. Phys. Chem. B* **2012**, *116*, 11791−11797. (b) Polyansky, D. E.; Muckerman, J. T.; Rochford, J.; Zong, R.; Thummel, R. P.; Fujita, E. *J. Am. Chem. Soc.* **2011**, *133*, 14649−14665.
(17) Bridgewater, J. D.; Lim, J.; Vachet, R. W. *Anal. Chem.* **2006**, *78*, 2432−2438.
(18) Wu, Z.-J.; Luo, S.-W.; Xie, J.-W.; Xu, X.-Y.; Fang, D.-M.; Zhang, G.-L. *J. Am. Soc. Mass Spectrom.* **2007**, *18*, 2074−2080.
(19) (a) Jackson, S. M.; Chisholm, D. M.; McIndoe, J. S.; Rosenberg, L. *Eur. J. Inorg. Chem.* **2011**, 327−330. (b) Beierlein, C. H.; Breit, B.; Paz Schmidt, R. A.; Plattner, D. A. *Organometallics* **2010**, *29*, 2521−2532.
(20) Henderson, M. A.; Luo, J.; Oliver, A.; McIndoe, J. S. *Organometallics* **2011**, *30*, 5471−5479.
(21) (a) Vikse, K. L.; Woods, M. P.; McIndoe, J. S. *Organometallics* **2010**, *29*, 6615−6618. (b) Vikse, K. L.; Ahmadi, Z.; Luo, J.; van der Wal, N.; Daze, K.; Taylor, N.; McIndoe, J. S. *Int. J. Mass Spectrom.* **2012**, *323*−*324*, 8−13.
(22) Sewell, L. J.; Lloyd-Jones, G. C.; Weller, A. S. *J. Am. Chem. Soc.* **2012**, *134*, 3598−3610.
(23) Dallanegra, R.; Robertson, A. P. M.; Chaplin, A. B.; Manners, I.; Weller, A. S. *Chem. Commun.* **2011**, *47*, 3763−3765.
(24) Sewell, L. J.; Chaplin, A. B.; Weller, A. S. *Dalton Trans.* **2011**, *40*, 7499−7501.
(25) Patiny, L.; Borel, A. *J. Chem. Inf. Model.* **2013**, *53*, 1223−1228.
(26) Wang, K.; Goldman, M. E.; Emge, T. J.; Goldman, A. S. *J. Organomet. Chem.* **1996**, *518*, 55−68.
(27) (a) Doran, S.; Achard, T.; Riera, A.; Verdaguer, X. *J. Organomet. Chem.* **2012**, *717*, 135−140. (b) Cadierno, V.; Díez, J.; García-Garrido, S. E.; Gimeno, J.; Pizzano, A. *Polyhedron* **2010**, *29*, 3380−3386. (c) Ahlquist, M.; Gustafsson, M.; Karlsson, M.; Thaning, M.; Axelsson, O.; Wendt, O. F. *Inorg. Chim. Acta* **2007**, *360*, 1621−1627. (d) Burk, M. J.; Harper, T. G. P.; Lee, J. R.; Kalberg, C. *Tetrahedron Lett.* **1994**, *35*, 4963−4966.
(28) Müller, T.; Badu-Tawiah, A.; Cooks, R. G. *Angew. Chem., Int. Ed.* **2012**, *51*, 11832−11835.
(29) (a) Bernskoetter, W. H.; Lobkovsky, E.; Chirik, P. J. *J. Am. Chem. Soc.* **2005**, *127*, 14051−14061. (b) Janak, K. E.; Parkin, G. *J. Am. Chem. Soc.* **2003**, *125*, 13219−13224.
(30) Zuidema, E.; Escorihuela, L.; Eichelsheim, T.; Carbó, J. J.; Bo, C.; Kamer, P. C. J.; van Leeuwen, P. W. N. M. *Chem.—Eur. J.* **2008**, *14*, 1843−1853.
(31) Zhu, G.; Janak, K. E.; Parkin, G. *Chem. Commun.* **2006**, 2501−2503.
(32) Pike, S. D.; Pernik, I.; Theron, R.; McIndoe, J. S.; Weller, A. S. *J. Organomet. Chem.* **2015**, *784*, 75−83.
(33) Hooper, J. F.; Young, R. D.; Weller, A. S.; Willis, M. C. *Chem.—Eur. J.* **2013**, *19* (9), 3125−3130.
(34) Brayshaw, S. K.; Harrison, A.; McIndoe, J. S.; Marken, F.; Raithby, P. R.; Warren, J. E.; Weller, A. S. *J. Am. Chem. Soc.* **2007**, *129*, 1793−1804.
(35) Lambert, J. B.; Greifenstein, L. G. *J. Am. Chem. Soc.* **1974**, *96*, 5120−5124.
(36) (a) Yang, H.; Gao, H.; Angelici, R. J. *Organometallics* **1999**, *18*, 2285−2287. (b) Blum, J.; Rosenfeld, A.; Gelman, F.; Schumann, H.; Avnir, D. *J. Mol. Catal. A: Chem.* **1999**, *146*, 117−122.
(37) Ingleson, M. J.; Mahon, M. F.; Weller, A. S. *Chem. Commun.* **2004**, 2398−2399.

DOI: 10.1021/acs.organomet.5b00322
Organometallics 2015, 34, 3021−3028

(38) Halpern, J.; Riley, D. P.; Chan, A. S. C.; Pluth, J. J. *J. Am. Chem. Soc.* **1977**, *99*, 8055−8057.
(39) Landis, C. R.; Halpern, J. *J. Organomet. Chem.* **1983**, *250*, 485−490.
(40) Hoops, S.; Sahle, S.; Gauges, R.; Lee, C.; Pahle, J.; Simus, N.; Singhal, M.; Xu, L.; Mendes, P.; Kummer, U. *Bioinformatics* **2006**, *22*, 3067−3074.

DOI: 10.1021/acs.organomet.5b00322
Organometallics 2015, 34, 3021−3028